Pressurized switching unit designed to start and to crowbar a turbulence heating experiment

G. Klement, G. Müller

IPP/4/52 June 1968

INSTITUT FÜR PLASMAPHYSIK

GARCHING BEI MÜNCHEN

INSTITUT FÜR PLASMAPHYSIK

GARCHING BEI MÜNCHEN

Pressurized switching unit designed to start and to crowbar a turbulence heating experiment

G. Klement, G. Müller

IPP/4/52 June 1968

The contents of this report will be presented at the 5th Symposium on Fusion Technology at St. Catherine's College, Oxford, 2nd - 5th July 1968.

Die nachstehende Arbeit wurde im Rahmen des Vertrages zwischen dem Institut für Plasmaphysik GmbH und der Europäischen Atomgemeinschaft über die Zusammenarbeit auf dem Gebiete der Plasmaphysik durchgeführt.

Contents:

Abstract

1. Introduction

2. Start spark gap
2.1 Development aspects
2.2 Electrode arrangement and trigger operation
2.3 Characteristics

3. Crowbar spark gap

4. Switching unit
4.1 Design and technological considerations
4.2 Electrical data
4.3 Operation in the turbulence heating experiment

Appendix

A1 Fast breakdown
A2 Potential diagrams of start gap arrangement
A3 Pulse breakdown voltage measurements

Literature

IPP 4/52

Pressurized Switching Unit Designed to Start and to Crowbar a Turbulence Heating Experiment

G. Klement, G. Müller

June, 1968

Abstract:

A start spark gap and a ferrite decoupled crowbar gap,moulded together in an epoxy resin pressure chamber of outer size 20 x 14 x 10 cm, are described.

The switch originally designed for switching the main bank of a 40 KV, 400 KHz turbulence heating experiment (1) (2) (3), and also used later for discharging the associated theta pinch preionization bank, could afford a wide range of application.

As arranged in this experiment, the main bank of which has a double transit time of only 20 nsec., the start gap must have a jitter of less than 10 nsec. over a range of about 1:3, when triggered by a 50 KV pulse voltage of 80 nsec. rise time. The inductance of the start gap is 35 nH, while the crowbar gap has a saturated inductance of 180 nH, which could be reduced by modifying the trigger circuit.The experience in testing and operating 60 units, with the associated trigger circuits and such data as delay, jitter, prefiring rate and stability to voltage transients, is reported.

Investigations on pulse breakdown, depending on trigger voltage characteristics up to ten atmospheres, and the influence of gap spacing will be discussed, with regard to spark gap development, in the Appendix of this report. Potential plots of some static and triggered cases will be given too.

1. Introduction

The development of the reported switching unit will be carried out primarily for the main bank of a turbulence heating experiment, which was projected to investigate the collisionless processes of fast theta pinches at lower densities.(1) The experiment, which is fully described at this conference (3) and earlier by Fertl et al. (2), demands a switching unit of low dimensions containing a start spark gap and a crowbar spark gap for switching the capacitor voltage of 40 KV with low jitter and wide switching range, because of the short transmission lines and the applied preionization means. Further requirements are the free selection of voltage polarity, the change of the supplied energy by the charging voltage and a high initial voltage rise. The aspects leading to the development and the construction of the switches had been already presented at the 4th Symposion at Frascati (4), discussing especially the ionization means to trigger a gap. The production of the demanded high frequency field of 11 KG, 450 KHz in the double fed coil, determined by experimental conditions up to 2 x 18.5 nH, is possible with 120 energy storage capacitors, which were available, if groups of two are switched together for starting and crowbaring. The specifications of the capacitor are 40 KV, 0.1 /uF and 80 nH, 140 mohm internal parameters. This also concures with the possibility of arranging the bank in the lab dimensions. Considering the cross section of the two capacitor cases of 40 x 13 cm and the restricted length in coil direction a limited room of 40 x 13 x 45 cm is available for the switching instruments, i.e. charging devices, trigger devices, spark gaps and transmission line connections. The design results in an assembly of two capacitors and a switching unit which all have a volume of 48 000 cm^3 (sizes 43 x 15 x 45 cm) together with the mentioned auxiliary means and are endowed with full dielectric holdoff to the surrounding whereas the switch unit itself is of outer sizes 20 x 14 x 10 cm (2800 cm^3).

The spark gaps have a rather low charge flow and current, so that current forces and erosion are not to be considered seriously. Therefore it seems to be appropriate to take aluminium as electrode material with the advantage of a lower work function and nonconducting erosion products. On account of the limited room available, it has been decided to design pressurized gaps which are known to have lower inductance and better ionization conditions. The additional factor is that the switch range can be adjusted by changing the pressure.

The start and crowbar spark gap operation and characteristics are given now in detail while the switch unit is discussed subsequently under technological and operational aspects.

2. Start spark gap

2.1 Development aspects

The construction of the start spark gap is outlined by the following conditions, presuming that the photo and field emission of the electrode surfaces reach a precise and fast breakdown. The auxiliary electrodes should,

1) not seriously distort the static field between the main electrodes (uniform static field),
2) produce a strong, more nonuniform trigger field and
3) ionization should originally occur on a small area of the surface of at least 2 electrodes, where a sufficiently large positive voltage gradient exists to accelerate the electrons
   and also
4) the influence of the erosion of those parts of the auxiliary electrodes which give the initial arc must be unimportant.

2.2 Electrode arrangement and trigger operation

The start spark gap has cylindrical electrodes (I,II) 30 mm in diameter and a parallel rod trigger electrode (III) 8 mm in diameter (Fig. 1). An irradiating gap (III-IV) formed by tungsten pins is situated inside the hollow trigger electrode and irradiates the switching gaps through holes 3 mm in diameter. The trigger electrode rod is arranged asymmetrical to the main electrodes, which possibly prevents erosion because of the current forces and decreases the gap inductance by reducing the total gap length. This displacement puts the trigger electrode in a region with an original weaker field, as will be discussed in the Appendix with regard to potential plots.(Fig. 15-18).

On the other hand, the trigger fields would not be influenced by the above, because they are only dependent on the curvature of the electrode surfaces and on the magnitude of the potential difference between them.

The circuit diagram of the start circuit, approximately effective in the turbulence heating bank, is represented in Fig. 1. The commen electrode is controlled by an ohmic divider at fourtenth (0.4) of the working voltage and is coupled to the irradiating pin by mean of R_1. With reference to Fig. 2 the trigger operation of the spark gap may be explained in the manner of the swinging cascade gap (5). The irradiating gap receives a trigger pulse, which causes breakdown between the pin and the trigger electrode with a certain jitter, satisfactorily decreased, if the short and nonuniform gap could be overvolted by a sufficient steep trigger pulse rise. Moreover, the breakdown time should be several times smaller than the time constant $R_1 . C_1$, which condition is expressed in terms of the steepness S (KV/nsec) and pulse breakdown voltage,

$$U_{pi}, \text{ as: } U_{pi}/S < R_1 . C_1$$

The potential of the trigger rod now becomes that of the trigger pulse and, if it is of opposite polarity to the charging voltage, it produces a strong, more nonuniform field in the first stage gap (look Fig. 2). The time constant of the trigger potential rise is indicated by the trigger cable impedance and the trigger electrode capacitance, $Z_t.C_1$, and so also partly determines the pulse breakdown voltage of the gap III - I, which breakdown is prepared by the provided start electrons. Now, the potential change of III is governed by the time dependent arc resistance, the capacitor inductance and resistance, the capacitor C_1 and the associated stray inductance of the circuit (5:p.122). Fig. 2 represents the operation of the trigger electrode. The upper oscillograms show the different voltage waveforms at the trigger electrode comparing the irradiated and the nonirradiated breakdown, the main capacitor charging voltage being zero. With a shorted irradiation gap, the breakdown to the main electrode occurs with a considerable spread and consequent jitter, while irradiation attains a steeper pulse, effected by sharpening, and breakdown with less jitter. The lower recordings present the trigger electrode voltage with charged capacitor. The reference lines are at 0.4 of the working voltage. The higher frequencies to be seen, are reflections due to the mismatched coil of the test circuit.

The total jitter is observed to be mainly dependent on the jitter of the first gap in the sequence of trigger operation. Therefore,it has to be considered whether the irradiating gap, as arranged in the present circuit, is of substantial advantage. It will be proved later that the consequent operation of the series connected irradiating gap and the gap being irradiated is of a problematic nature, because of the difficulty of adjusting the irradiating gap to a constant and low breakdown voltage at higher pressures. Also stray capacitances and inductances of the electrodes and connected circuits have to be observed carefully for resonance

oscillations, which could seriously upset exact breakdown. Hence, a more successful arrangement could be attained by a steeper trigger waveform and by means of field emission (6, 7, 8) or with parallel connected irradiating gap (9).

2.3 Characteristics

In view of Fig. 4, the jitter and delay data of the gap versus pressure are discussed. The data are recorded during life test of a model circuit connected to a double fed coil under bank operational conditions. The upper and lower diagrams show the delay time and jitter of the switch at constant working voltages.

The delay time is defined here as the time which elapses from the start of the trigger voltage rise to the instant when the 50 % value of the capacitor voltage appears at the output of the spark gap. With regard to this definition the trend of the delay can be explained primarily with increasing trigger pulse breakdown voltage of the first stage gap with increasing pressure. In this range the jitter is constant and determined by the irradiating gap. Further increase of pressure results in a more and more less overvolted second stage gap, because the maximum overvoltage there is only less than the double working voltage (5). At the very low working voltages, interference of the consequent breakdown of the irradiating gap and the first stage gap possibly limits the switch range.

The somewhat lower time data of negative charging voltages are stated by the better ionization conditions in the surrounding of the irradiating holes, being of use only for the negative charging voltages. At the higher charging voltages the ionization conditions seem to be made more equal by increased influence of field emission. Fig. 6 finally shows the jitter depending on discharge number during life test.

The stability of voltage transients is plotted in fig. 5. This characteristic is mainly dependent on the dynamic

behavior of the common electrode and the irradiating gap. With regard to the schematic circuit diagram (Fig. 5), the time constant of this gap, formed by R and the gap capacitance, is responsible for unwanted ignition, if the transient voltage rise is of similar magnitude. On the other hand this time constant cannot be reduced below a certain value, depending on the mentioned trigger operation requirements. The common electrode itself could be controlled perfectly by the capacitor divider C_1 and C_2 with the disadvantage of a more direct coupling to the irradiating gap. Therefore it is preferable to overvolt the second stage gap more than the first stage in order to avoid the ignition of irradiation. Three cases of transient controlling have been investigated with the waveform recorded schematically in the figure.

In fig. 3 photographic views of the discharge are shown in order to explain the visible erosion distributed over nearly the whole length of the cylindrical electrodes. The left part of the figure represents sequences of five discharges, above recorded single and below another sequence recorded together. It seems noteworthy that the arc is formed at different spots and sometimes the discharge possibly burns like an interrupted arc , as also mentioned by Menke (10). The right-hand part of the figure presents additional discharge views at a higher pressure. Pillsticker and Hintz (11) suppose precorona discharges during the charge period, which could not be refused with regard to some visible gleams at the spheric extensions of the main electrodes.

3. Crowbar spark gap

The crowbar spark gap is of the ferrite decoupled type, a principle first mentioned by Früngel et al. (12) and subsequently treated at length in the literature (13, 14, 15, 16, 17, 18). Therefore only a short description is necessary, with regard to fig. 1, showing the gap arrangement and the crowbar circuit and to fig. 7, which demonstrates the operation of the crowbar gap.

The crowbar spark gap is arranged at right angles to the start spark gap, formed by a spherical extension (II) of the grounded start gap electrode (40 mm in diameter) and the decoupled cylindrical crowbar electrode (V) (30 mm in diameter), which also receives the crowbar trigger pulse from the spherical pulse sharpening electrode (VI) (20 mm in diameter). The coaxial ferrite cores are located outside the pressure chamber and form a coaxial tube of about 300 mm length and 10 / 60 mm in diameter. (Fig. 1). According to this, the crowbar branch inductance is of 180 nH in the saturated state. Its unsaturated inductance will be about three magnitudes higher.

During the risetime of the trigger pulse at the pulse sharpening electrode, the ferrite cores are premagnetized to a fraction of minus Φ_s (saturation flux), so that the peak value of the very fast voltage rise at the crowbar electrode (V) is determined approximately by

$$U_{c\ max} = \sqrt{2.\ \Phi_s.\ s}$$

Φ_s saturation flux (KV.ns)
s steepness of U_c (KV/ns)

To trigger the crowbar gap, the pulse breakdown voltage has to be less than $U_{c\ max}$, otherwise the voltage of the crowbar electrode would fail owing to the low impedance of the saturated ferrite cores. At correct operation this is done by the coil current.

The coaxial tube, presenting a single wound coil, is filled with 30 ferrite cores of 50 / 15 mm in diameter and 10mm width and forms a transient impedance of approximately 200 ohms in the unsaturated state. The double saturation flux is about 6000 KV.nsec.

The waveforms for triggering the crowbar gap are recorded in fig. 7. With the steepness of 0.5 KV/ns shown at the pulse sharpening electrode, $U_{c\ max}$ would be only

$\sqrt{-3000} = 55$ KV

but with the help of the pulse sharpening gap, the steepness of the crowbar electrode voltage rise is about 1.5 KV/ns, so that $U_{c\ max}$ would be $\sqrt{9000} = 95$ KV

The jitter to be seen in the oscillogram (Fig. 7) is caused by the breakdown spread of the pulse sharpening gap, which could be avoided, if necessary by irradiation of the gap. The slow positive voltage rise at the beginning is generated by the premagnetization circuit, whose current is limited by the resistance R_2 (Fig. 1) to a suitable value depending on ϕ_s.

The load currents for uncrowbared, crowbared and diverted operation are recorded during the life test with two model circuits connected to a double fed coil. The crowbar ripple is 15 %, as defined in (14), ripples in the diverted case are 50 %, the height of which depend on the crowbar branch and capacitor inductances. The constancy of operation seems to be satisfactory.

The crowbar branch inductance could be reduced, if wanted, by modifying the trigger pulse steepness, resulting in a lower number of necessary ferrite cores and/or by use of another type of ferrite core with an increased ratio of outer to inner diameter (15).

4. Switching unit

4.1 Design and technological considerations

On account of the limited room available for the switching devices and the decisions to provide

a) the ferrite decoupled crowbar switch
(originally developed as a component of the 2.5 MJ Bank at Garching)

b) short strip lines as energy transmission lines

and further with regard to the former mentioned conditions, a pressurized switch unit as a combination of start and crowbar switch is in place.

Fig. 8 gives a photograph of the device; fig. 9 shows it

together with the energy storage unit to switch. The topological structure and the idea of the arrangement are explained with regard to the schematic drawing (Fig. 10).

The start spark gap, as described above, and the ferrite decoupled crowbar gap are mounted together in an epoxy resin chamber with a perspex cover. Because of the nature of the capacitor bushings and the energy stripline design, the unit is of the strip line design too. By this means, all three components form one assembly.

The grounded part of the stripline, considerably extended (Fig. 10), forms the bottom of the pressure case and is embedded in the resin. This plate also supports the connector flange for the outer part of the coaxial ferrite tube, which should be best mounted parallel to the stripline, because of it's being the most extended individual part.

The other stripline parts bear the start electrodes which form the start spark gap.

The stripline parts are made of aluminium and insulated by foils. The necessary bushings for the trigger and pressure connections located at both sides of the case are of the same material because of the better bonding to epoxy resin.

The epoxy resin is of the two - component type and filled with quartz. The fresh mixtures are degassed with a large surface at 1 torr and cast in the prepared aluminium mould at 40 torr. The final process is finished after a moulding time of 12 h and an ageing time of 7 days at 60°C. This procedure results in satisfactory dielectrical and mechanical properties.

The outer static hold off of the unit, now being 50 KV, may be increased by extending the stripline connections. The inner hold off, determined by the stripline part insulation is measured to be greater than 80 KV. The maximum attainable static pressure is proved to be 16 ATM overpressure, but, with regard to safety, an operational pressure not higher than 10 ATM is recommended.

The pressure chamber operates with a clean, dry (-50^{o} C dew point) mixture of 80 % N_2 and 20 % O_2, so-called artificial air, which is stocked in bottles and commercially available with constant quality. This seems to be of some importance, because of uncontrolled humidity causes, increased erosion and conducting erosion products, premature breakdown and subsequently decreased life.

If the pressure chamber is supplied with normal compressed air from the pressure line and if the air is changed, after each discharge premature breakdowns happen and the used gas is of pungent smell. Investigations of discharges in pure nitrogen (19) have shown that in the presence of water vapour great quantities of oxides are generated, with the result that the breakdown voltage of the mixture is heavily decreased.

4.2 Electrical data

With the gap spacing of fig. 1 and the conditions given below in detail, fig. 11 shows the DC-breakdown voltage of all gaps dependent on the pressure. A minimum working voltage with a litter less than 6 nsec absolute can be observed (broken line) as important operational characteristic. This is in accordance with the jitter data versus pressure plot (Fig. 4) and is valid under the mentioned trigger pulse conditions.

If the switching unit is mounted together with the two capacitors of the described type, inductance of which could be reduced by a special stripline connection, the data of the assembly are as follows:

charging voltage	40 KV
outer hold-off voltage (assembly)	50 KV
inner hold-off voltage (switch unit)	>80 KV
stored and switched energy	160 J
max. discharge current at 1.4 MHz, 40 KV	70 KV
operational discharge current at 440 KHz, 40 KV	22 KA
charge flow of start gap, reversed operation	0.08 C

charge flow of crowbar gap, crowbared operation	0.24 C
inductance of the start spark gap x)	35 nH
inductance of the crowbar gap x) with saturated ferrite tube	185 nH
inductance of the assembly	65 nH
resistance of the assembly	85 mohm

x) in between stripline connections

During development three units were tested for up to 10^4 and $0.5 \cdot 10^4$ discharges under bank operational conditions, the parameters remaining nearly unchanged. The erosion products of the aluminium electrodes are a nonconducting white coloured powder if humidity is absent. However, lifetime under bank operational conditions with the exchange of one third of the volume after each discharge had been found to be of the order of 10^4. The behavior of aluminium at higher currents remains untested but is under investigation (20).

The premature ignition rate seems to be very low. It could not be decided, whether occasional breakdowns are caused by the switching unit itself or by the trigger circuits.

4.3 Operation in the turbulence heating experiment

60 switching units and 120 energy storage capacitors are mounted together to form the main and theta pinch preionization bank of the turbulence heating experiment. The experiment has been in operation since March 1967 without noticeable interruption.

Fig. 12 shows side views of the completely installed switching units showing also the wooden tiers,, the whole trigger equipment and the pressure supply. Each unit possesses its own shorter, not visible but mounted at the bottom of the capacitors.

Fig. 13 presents oscillograms of simultaneous operation of 60 units, recorded at the experiment. Explanations are given

in the figure. The voltage rise at the coil is measured without RC suppressor units . During operation (approximately 3000 discharges) major trouble of the switching units and associated circuitry does not occur.

Fig. 14 gives an impression of the visible erosion taken from a demounted sample. Main erosion spots are in the regions near to the irradiation area, denoted by a., and at the crowbar gap b., both areas being coloured greyish black.

Appendix

A1 Fast breakdown

The problems of fast breakdown of a gas are treated at length in the literature and there is a series of standard books (21, 22, 23, 24) for the reference of the switch engineer. The research on ionization growth leading to the breakdown of a gap is done by electrical and photographical methods (i.e. 22), which are sometimes not easy to compare with the methods of oscillograpic voltage recording. This is mainly the method used by the engineer. Ionization growth parameters and mechanisms usually investigated under static field or under pulsed conditions, with a very steep front and a flat, constant plateau.

Fast breakdown, as it has been called in this report, needs some more explanation which will be given by its dependence on the following terms.

1) Provision of start electrons by irradiation or field emission from the cathode surface to be undependent of statistical fluctuations. (Parameter and constants of technical use seem to be fairly unknown and are of a very approximate character.)

2) Townsend's first ionization coefficient, α, which itself has a statistical value too and is mainly determined as a function of the ratio E/p in uniform fields. It is also dependent on other parameters, in a more complex manner, as described by the theory of electron impact. Further attachment and detachment coefficients are of main importance too and seem to be dependent on p and E/p in a different way as α.
If $(\alpha . x) > 20$ (e.g. 22, p. 79) limits the requirement of fast ionization growth as explained by Raether, Loeb and Llewellyn-Jones and if an $\alpha_{eff.}$ is defined by $\alpha_{eff.} = \alpha - a$ (a: attachment coefficient), it is of great importance that α gains more influence at higher pressure (24, p. 76), so that E/p could be saved with the consequence of lower trigger voltage.

3) The secondary coefficient, which could only be the secondary photonelectric interaction with the gas, assuming a single avalanche breakdown. The dependencies of this mechanism are summarized as follows: Photon energy is an increasing function of E/p and depends also on possible exited states of the neutrals. The absorption depends on photonenergy and inversely on the pressure (22, p. 44).

The above mentioned dependencies are not easily attainable by the engineer, within the critical spark gap range of pd=1000to.3000 Torr.cm(p=700 to 7000 Torr) and subsequently, E/p=200to 600 V/cm Torr for various gases. There is also little information available on larger overvoltage (25) or an approximately linear rising applied field, because the instrument of triggering a gap is usually steep voltage rise in the range of more than 0.5 KV/ns. Two questions are of a very importance:

a) Are breakdown times lower than the known electron gap transit times explained by a single avalanche theory

assuming space charge field distortion (e.g. by Raether and Loeb) or possibly explained by Llewellyn-Jones (24, p.74) and Ward (26), further in (21, 22, 23, 24, 27) .

b) Are there possibly interactions between great avalanches because of different time lags, if one or more start electrons are provided (28, 29, 22).

Summarizing it may be said that breakdown with times of the magnitude of electron gap transit times are not explained uniformly in the literature and data seem not to be available in technical ranges of requirements, in spite of great importance for triggered gaps.

A2 Potential diagrams of start gap arrangement

Fig. 15 - 18 represent potential diagrams of the gap arrangement of the start spark gap, measured at a two dimensional carbon paper model in order to discuss the electric field strength dependency on trigger field displacement. From fig. 15, the usual location of hypothetical trigger electrode will be defined as lying on the common diameter of the main electrode circles. With constant spacing, the common electrode could have no extension, otherwise it would lead to field distortion in the static case. In the process of triggering (see fig. 17) a very high field strength at the hypothetical triggerpin is generated but, the mean value of E should not be of the magnitude to ensure fast ionization growth. On the other hand a very thin electrode, curved like the potential surface, will not distort the static field too, but will only change the field strength by the magnitude of the trigger voltage. So a real trigger electrode of a certain crosssection is displaced preferably to avoid extension of total gap length and distortion of the original field, with regard to fig. 16, the maximum field strength of which is only increased weakly by about 10 %. In the triggered state, chosen so that first and

second stage gaps are overvolted by equal amounts which depend on the gap ratio, the mean field intensity is according to the trigger voltage magnitude. However the maximum field intensity is a function of the electrode surface curvature. The ratio of maximum to the mean value is increased by 1.1 to 1.4 if the plots would be exact.

It could be expected that such an optimum ratio exists originally causing fast ionization growth by increased $E/_p$ and further space temporal development of the current growth at decreased ionization conditions, possibly on account of spare charge distortion field. This possibility is discussed by Gruber (30) and in (11a).

A3 Pulse breakdown voltage measurements

The breakdown voltage of a linear rising pulse voltage of 1.3 KV/ns is investigated for various spacings, at a part of the gap arrangement, formed by the trigger electrode, the irradiating gap and one main electrode. Results are represented in fig. 19 and fig. 20, the latter showing the investigated circuit, an oscillogram of the pulse wave form and a plot of the mean breakdown field versus pressure. From fig. 19 a comparison of these results with the earlier data of Fletscher (29), Hancox and Goodall (31, 32) and Gruber (30) is attainable. The diagram is a plot of $\frac{V}{p \cdot d} = \frac{E \text{ mean}}{p}$ versus p.d which functional dependence is taken from the presentation of electron attachment controlled alternating field breakdown.

According to Brown in (33), the breakdown condition is of the type $\frac{\alpha}{P} = \frac{\beta}{P} + \frac{A}{(E/p)(p.d)^2}$

α Townsend's coefficient

β attachment coefficient

A parameter depending on electron energy distribution and velocity.

With regard to the circuit diagram (Fig. 20) the breakdown voltage at static and pulsed conditions, latter with the mentioned constant steepness, are recorded with and without irradiation while varying the parameter R and C of the circuit.

The lowest breakdown spreads over the whole pressure range are attained with R = 200 Ω and C = 125 pF, which both form a time constant of similar steepness like the originally applied pulse. The pulse operates the trigger electrode like described in part 2.2.

With decreased R high frequencies are generated in the gap circuit, consequently followed by an increased breakdown spread. With decreased C the stray capacitors of both gaps, which are of similar magnitude, are effective as potential divider. Then subsequently the irradiating gap occurs to breakdown at a considerable late instant of the applied pulse front and besides of being like a pulse sharpening gap, causes interference of the both series connected gaps.

The mean value of breakdown field strength with irradiation shows a strong linear dependency on pressure but increased field strength with decreased spacing.

The comparison of the $E/_p$ values with suitable data of the mentioned earlier investigations from fig. 19, results in a satisfactory agreement, proving also the assumption that weakly nonuniform fields would be an advantage with regard to lower trigger magnitude. The increased $E/_p$ values of Handox and Gruber could be explained by assuming a steeper voltage front.

The irradiated $E/_p$ values of the discussed arrangement forms the lower limit of the non-irradiated values with wide spread. This lower limit is not always touched. That proves only the statistical character of breakdown and the limited number of recordings (10 pulses).

With the help of ciphers, written near the breakdown spreads

it is noteworthy that the spread in E/p is considerably decreased with increasing pressure at constant spacing (possibly on account of field emission), but also seems to be weakly reduced with increasing p.d.

Literature:

1 E. Fünfer; Rep. 1/70, 1967, IPP Garching

2 K.H. Fertl, G.Herppich, A. Knobloch, H. Schlageter; Rep. 4/26, 1966, IPP Garching

3 G. Herppich, A. Knobloch, G. Müller; Rep. 4/ , 1968, IPP Garching

4 H. Häglsperger, G. Klement, R.C. Kunze, G. Müller; Rep. 4/28, 1966, IPP Garching

5 R.A. Fitch, N.R. McCormick; IEE Paper No. 3108, Nov. 1959

6 A.E. Bishop, G.D. Edmonds; Unpubl. Communication, Culham Laboratory

7 P.M. Barnes, J.E. Gruber, T.E. James; Rep. CLM - R 71, 1967, Culham Laboratory

8 A.E. Bishop, G.D. Edmonds, J. Sheffield; J. SCI. INSTRUM., Vol. 39, pp. 566 - 568, Nov. 1962

9 J.E. Gruber; Rep. 4/37, 1966, IPP Garching

10 H. Menke; ETZ (A) 87, H.10, p. 323, 1966

11 M. Pillsticker; ETZ (A) 89, H.2, p. 44 - 45, 1968

11a G. Goldenbaum, E. Hintz ; PIG 1962

12 E. Früngel, G, Röder; Verhandl. No. 213,1963

13 R. Wilhelm, H. Zwicker; Z. angew. Physik 19, p. 428, 1965

14 J. Gruber, G. Müller; Rep. 4/27, 1965, IPP Garching

15 G. Klement, R.C. Kunze, E.v. Mark, H. Wedler; Rep. 4/59, 1968, IPP Garching

16 E.v. Mark, H. Wedler; Rep. 4/59, 1968, IPP Garching

17 E.v. Mark, H. Wedler; Rep 4/54, 1968, IPP Garching

18 G. Klement, A. Knobloch, R.C. Kunze, G. Nützel, H. Schlageter; Rep. 4/58, 1968, IPP Garching

19 F.Boylett PIG 1?63 p.317

20 J. Gruber, R. Suess; 5th Symposium on Fusion Technology

21 L.B. Loeb, "Basic Processes of Gaseous Electronics", Los Angeles, 1960

22 H. Raether; " Electron Avalanches And Breakdown in Gases", London, 1964

23 F. Llewellyn-Jones; "Ionization And Breakdown in Gases", London, 1966

24 F. Llewellyn-Jones; "Ionization Avalanches And Breakdown", London, 1967

25 J. Dutton, S.C. Haydon, F. Llewellyn-Jones; Brit. J. Appl. Phys., 4, 1953

26 A.L. Ward (Harry Diamond Lab.) PIG, Paris, 1963

27 W. Köhrmann; Z. Naturforschg. 19a, 920 - 933,1964,

28 G.A. Mesjatz, Y.I. Bichkov, A.M. Iskol'Dsikij; PIG 210,1967

29 R.C. Fletcher; Phys. Rev. 76/10, 1949

30 J.E. Gruber, T.E. James, F.J. Kivlin; PIG 208, 1967

31 D.H.J. Goodall, R. Hancox; "Formative Time Lags in a Pressurised Spark Gap", Rep. Culham Lab., V B 22

32 D.H.J. Goodall; Rep. CLM - M 18, 1962

33 F. Llewellyn-Jones in FLÜGGE, HDP,Bd. XXII, 1956, p. 566 - 568

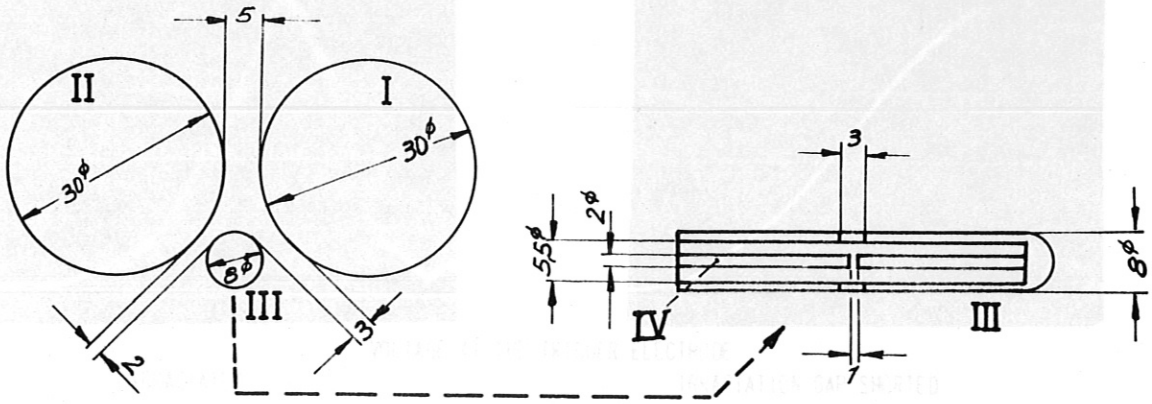

GEOMETRY OF START GAPS

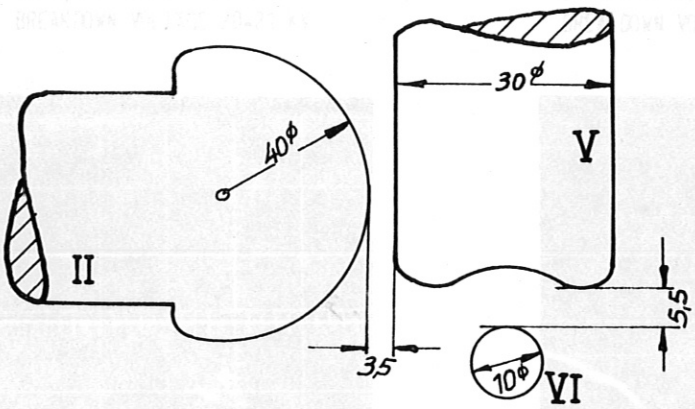

GEOMETRY OF CROWBAR GAPS

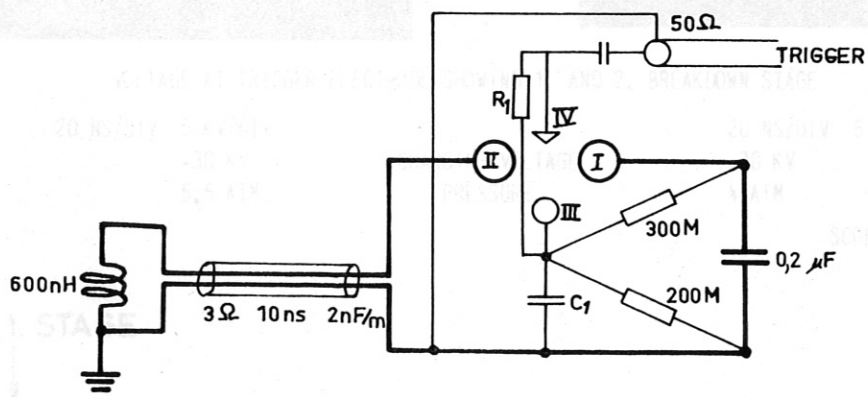

START CIRCUIT

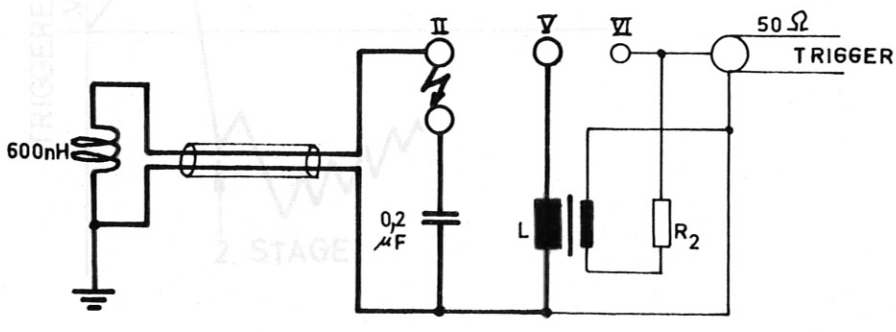

CROWBAR CIRCUIT

Fig. 1 CIRCUIT DIAGRAM AND GEOMETRY OF SWITCHING GAPS

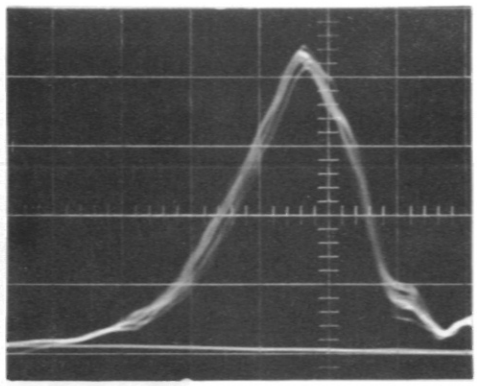

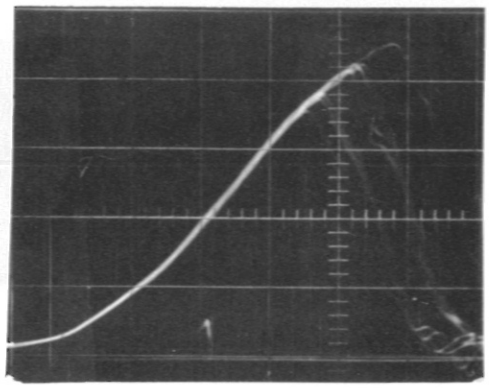

VOLTAGE AT THE TRIGGER ELECTRODE

IRRADIATED

20 NS/DIV 4,8 KV/DIV
JITTER OF IRRADIATING GAP 6 NS
JITTER OF BREAKDOWN 4 NS
BREAKDOWN VOLTAGE 20-21 KV

IRRADIATION GAP SHORTED

20 NS/DIV 6 KV/DIV

JITTER OF BREAKDOWN 26 NS
BREAKDOWN VOLTAGE 21-27 KV

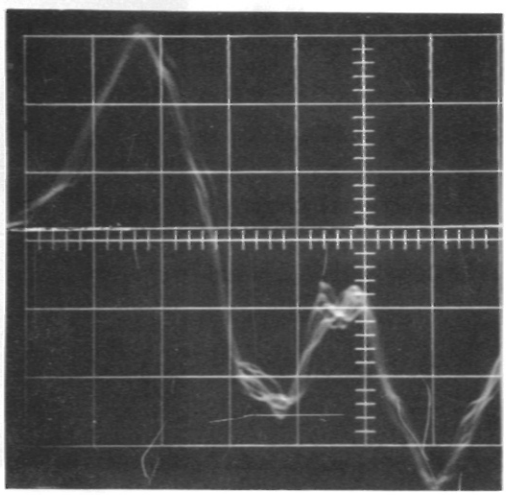

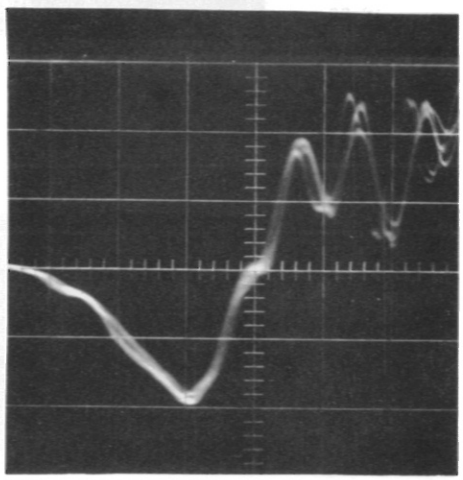

VOLTAGE AT TRIGGER ELECTRODE SHOWING 1. AND 2. BREAKDOWN STAGE

20 NS/DIV 5 KV/DIV
-30 KV
5,5 ATM

CHARGING VOLTAGE
PRESSURE

20 NS/DIV 8 KV/DIV
+30 KV
4 ATM

SCOPE JITTER 5 NS

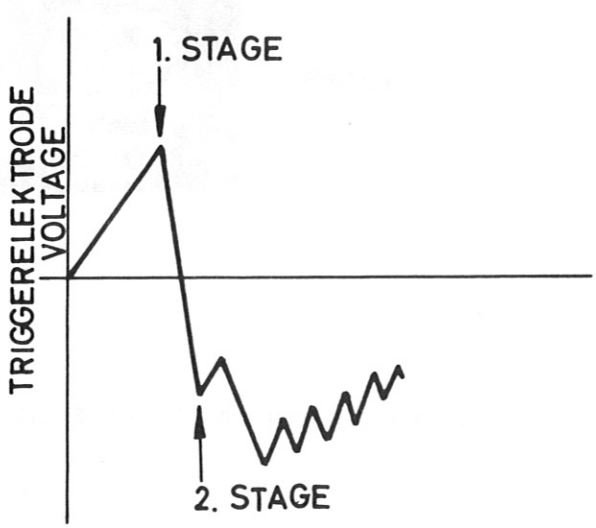

SCHEMATIC OF SPARK GAP BREAKDOWN

Fig.2 OPERATION OF THE TRIGGER ELECTRODE

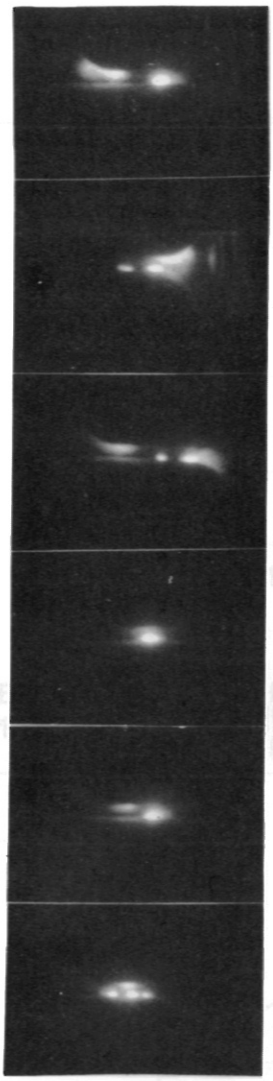

5 ATM
40 KV
20 KA
1 DISCHARGE

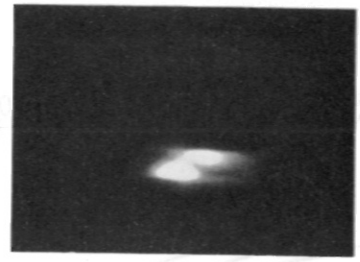

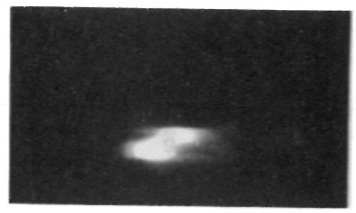

7 ATM
40 KV
20 KA
1 Discharge

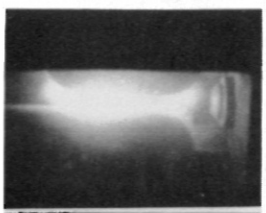

SEQUENCE OF
5 DISCHARGES

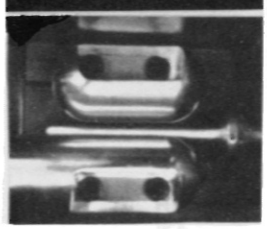

POSITION

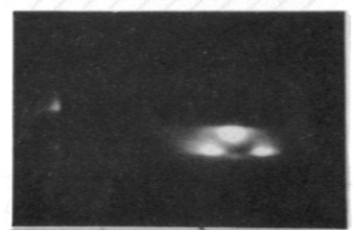

4 ATM, 40 KV, 20 KA
1 DISCHARGE

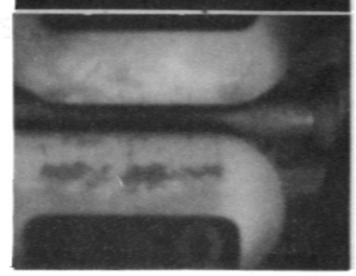

POSITION

Fig. 3 PHOTOGRAPHIC MAPPING OF START SPARK GAP DISCHARGE

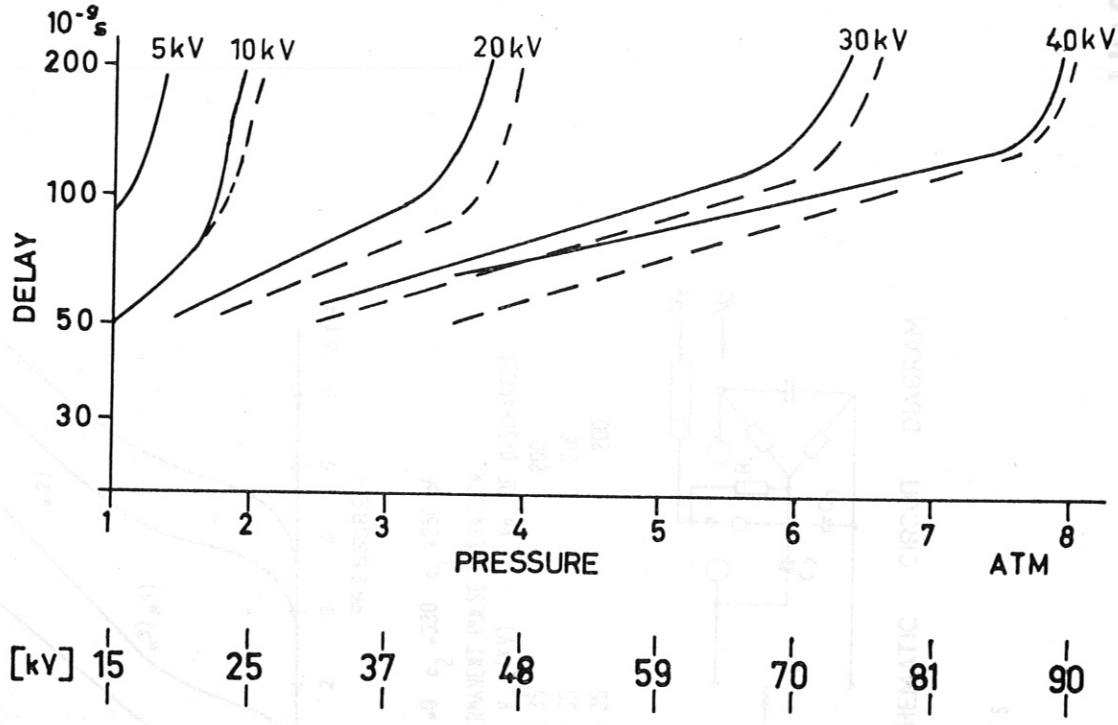

DC-BREAKDOWN AT PRESSURE [kV] 15 25 37 48 59 70 81 90

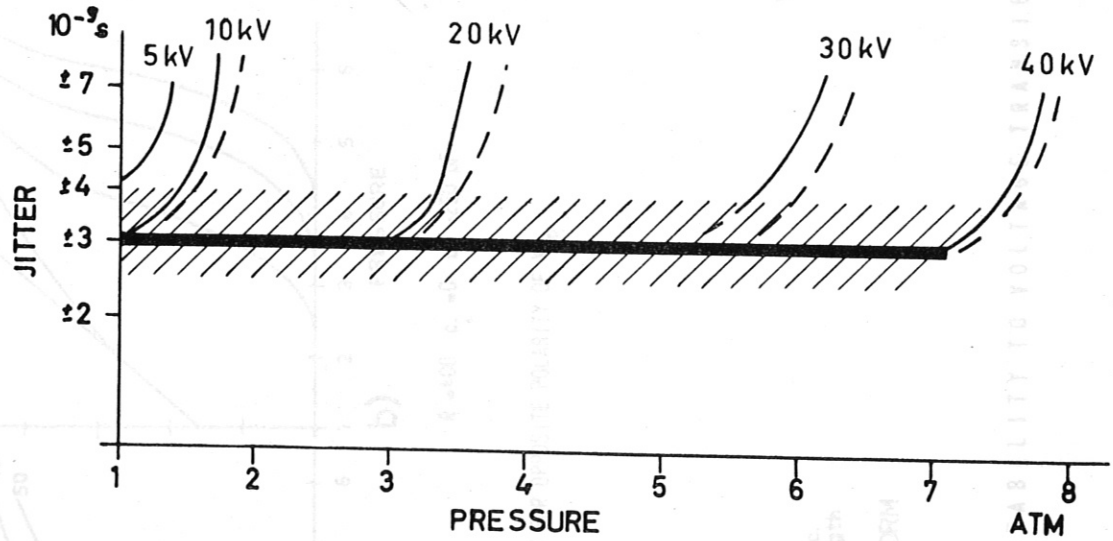

POS. ----
NEG. ——
WORKING VOLTAGE CONST = 5; 10; 20; 30; 40 KV
TRIGGER PULSE VOLTAGE 40 KV 100 NS RISETIME
SHADOWED REGION GIVING SPREAD OF OTHER MEASUREMENTS
DELAY TIME INCLUDING RISETIME OF TRIGGER PULSE

SCOPE JITTER 5 NS

Fig. 4 JITTER AND DELAY OF START SPARK GAP VERSUS PRESSURE
DERIVED FROM TWO SPARK GAPS AFTER 7 000 DISCHARGES 0,2 µF 40 KV

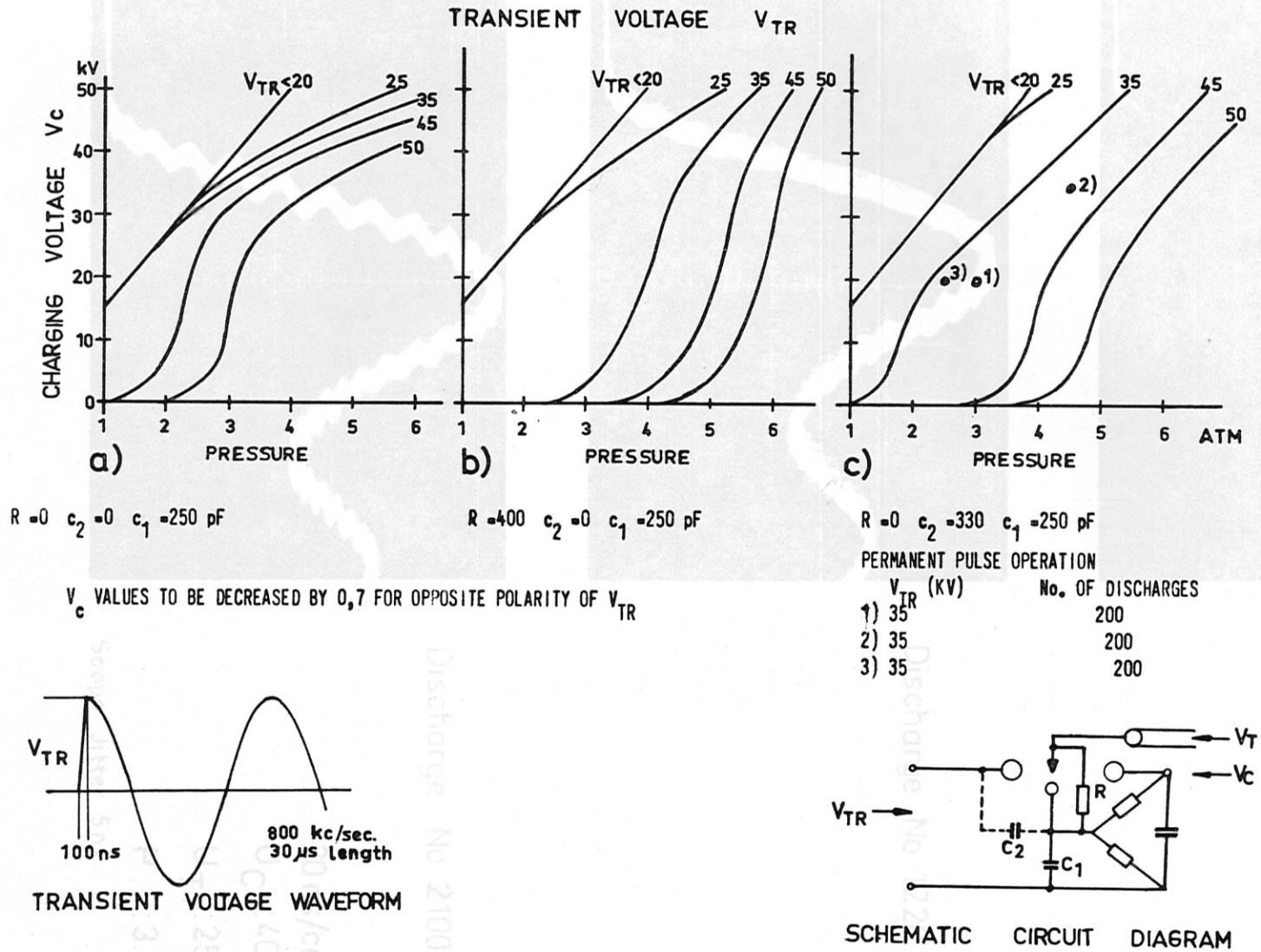

Fig. 5 STABILITY TO VOLTAGE TRANSIENTS

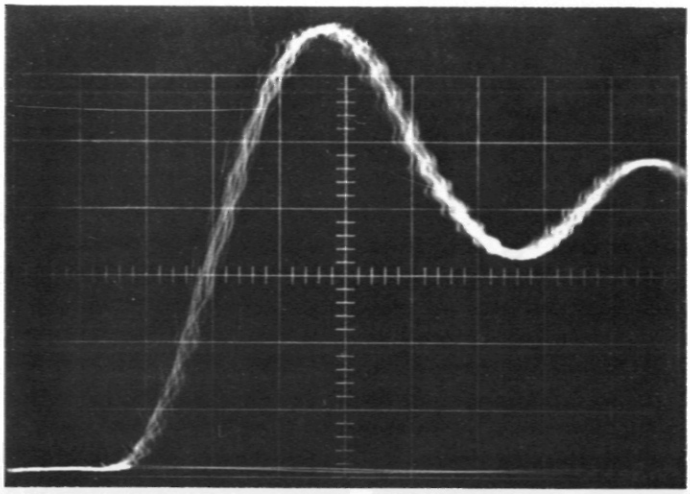

Discharge No 1.....30

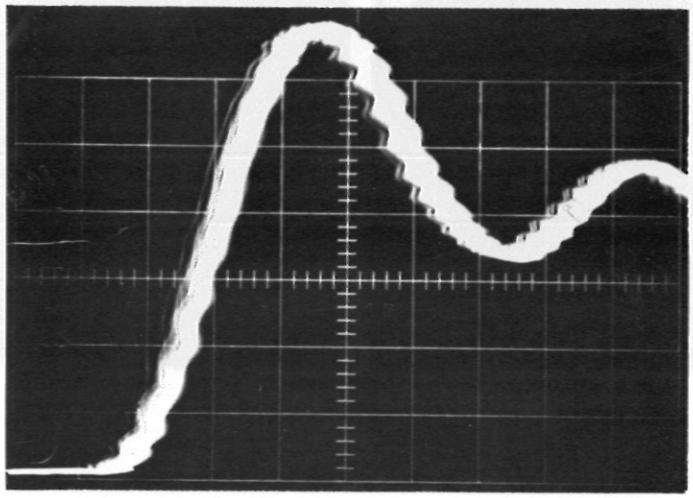

Discharge No 1220.....1470

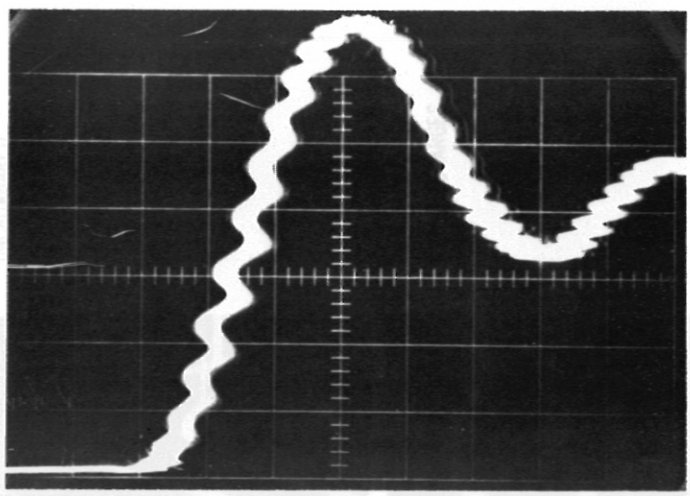

Discharge No 2100.....2500

20 ns/cm
U_C : 40 kV
U_T : 25 kV
P : 3.....3,5 atü

Scope Jitter 5 ns

Fig. 6 JITTER OF THE START SPARK GAP DURING LIFE TEST

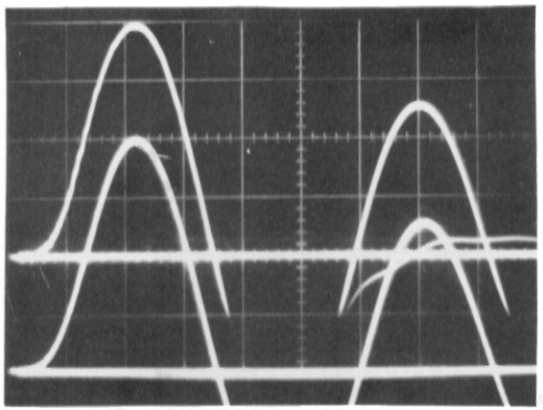

UNCROWBARED
100 DISCHARGES

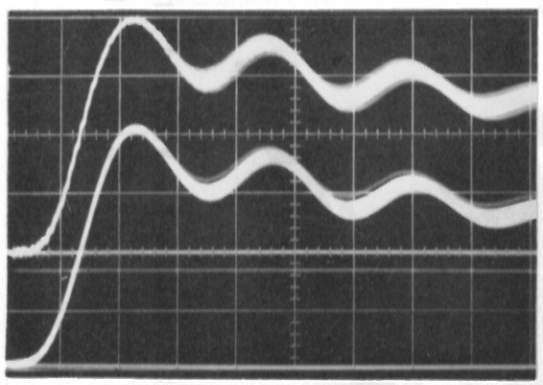

CROWBARED
100 DISCHARGES

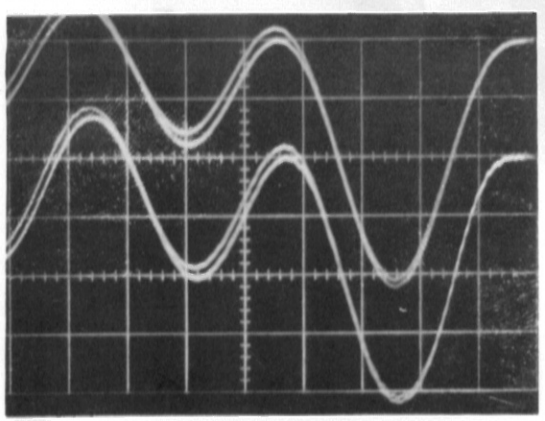

DIVERTED
20 DISCHARGES

LOAD CURRENT OF 2 UNITS CONNECTED TO DOUBLE-FED COIL
500 NS/DIV 5 KA/DIV

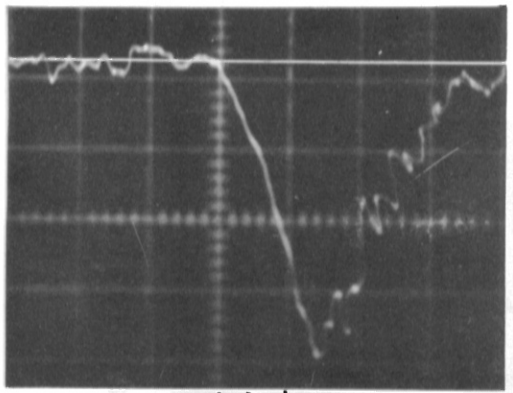

PULSE AT SHARPENING ELECTRODE
50 NS/DIV 19 KV/DIV
80 KV PEAK
70 NS RISETIME

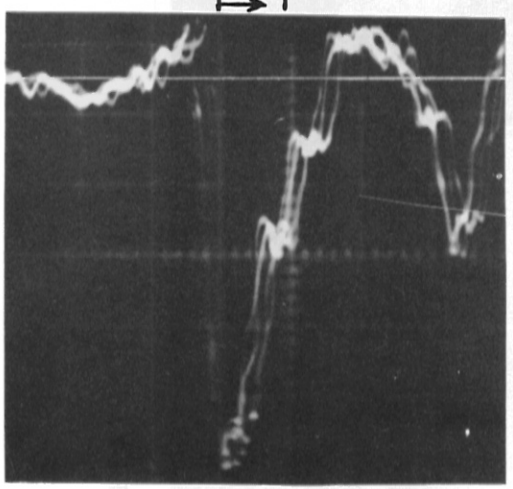

PULSE AT CROWBAR ELECTRODE
100 NS/DIV 14 KV/DIV
78 KV PEAK
20 NS RISETIME
NO DISCHARGE TO GROUND

CROWBAR TRIGGER PULSE
100 NS/DIV

Fig. 7 OPERATION OF THE FERRITE DECOUPLED CROWBAR SPARK GAP

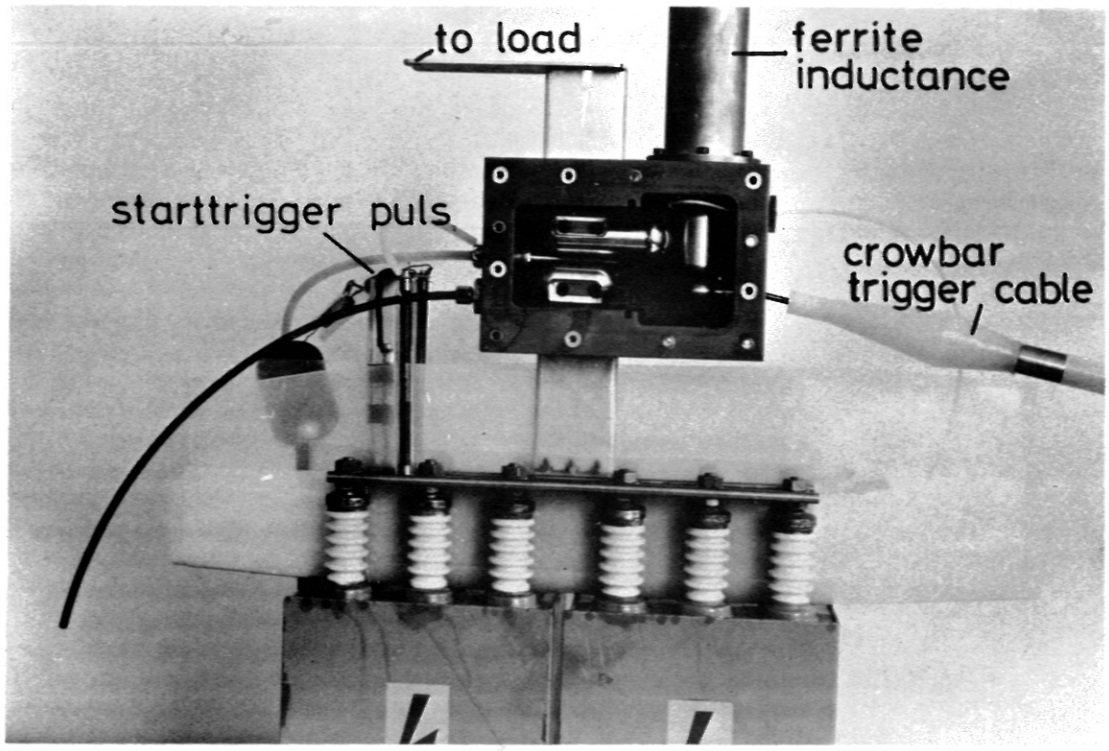

Fig.9 SWITCHING UNIT MOUNTED ON CAPACITORS 40 KV 0,2 µF

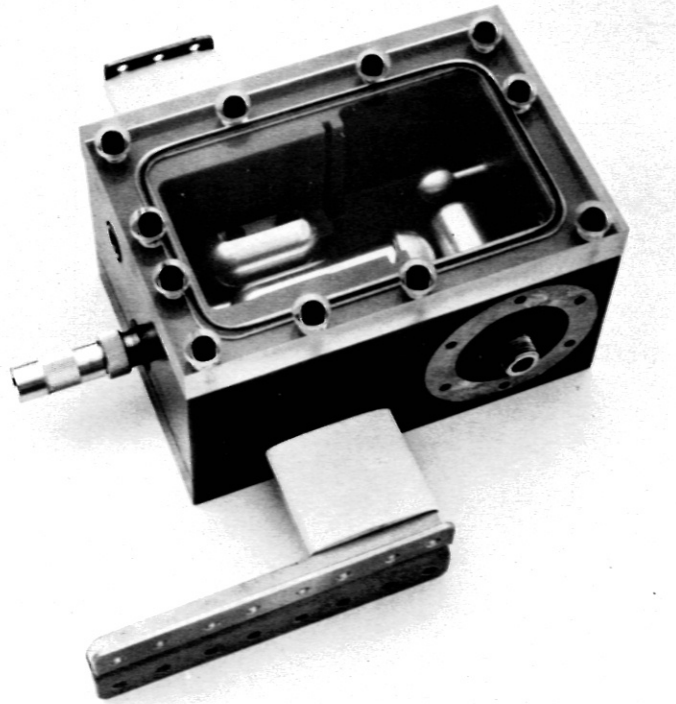

Fig. 8 PHOTOGRAPHIC VIEW OF SWITCHING UNIT WITHOUT COAXIAL FERRITE INDUCTANCE

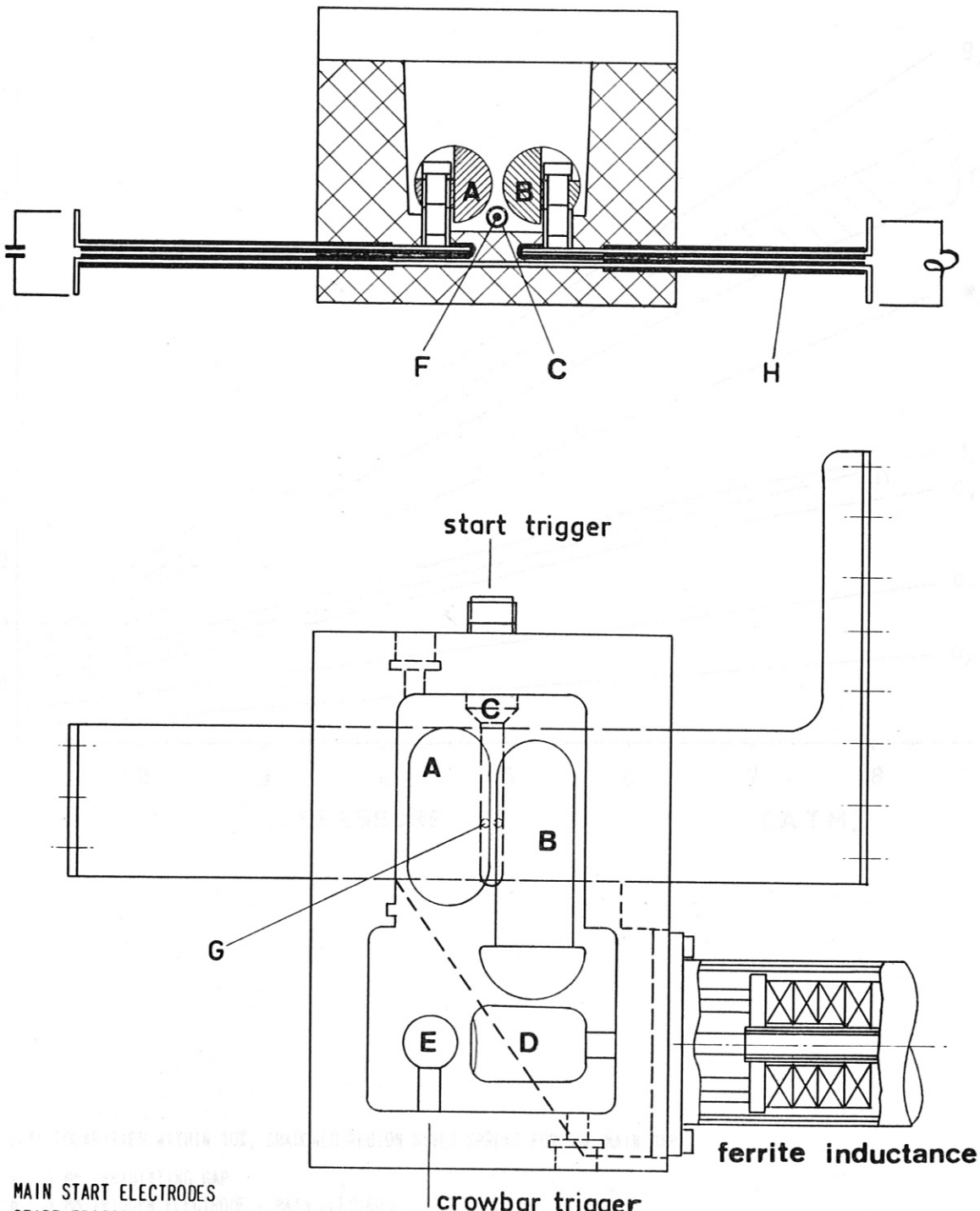

A,B MAIN START ELECTRODES
C START TRIGGER ELECTRODE
B,D MAIN CROWBAR ELECTRODES
E CROWBAR TRIGGER PULSE SHARPENING ELECTRODE
F IRRADIATING ELECTRODE WITH IRRADIATING APERTURE G
H STRIPLINE INSULATION (FOILS)

Fig. 10 SCHEMATIC DRAWING OF SWITCHING UNIT

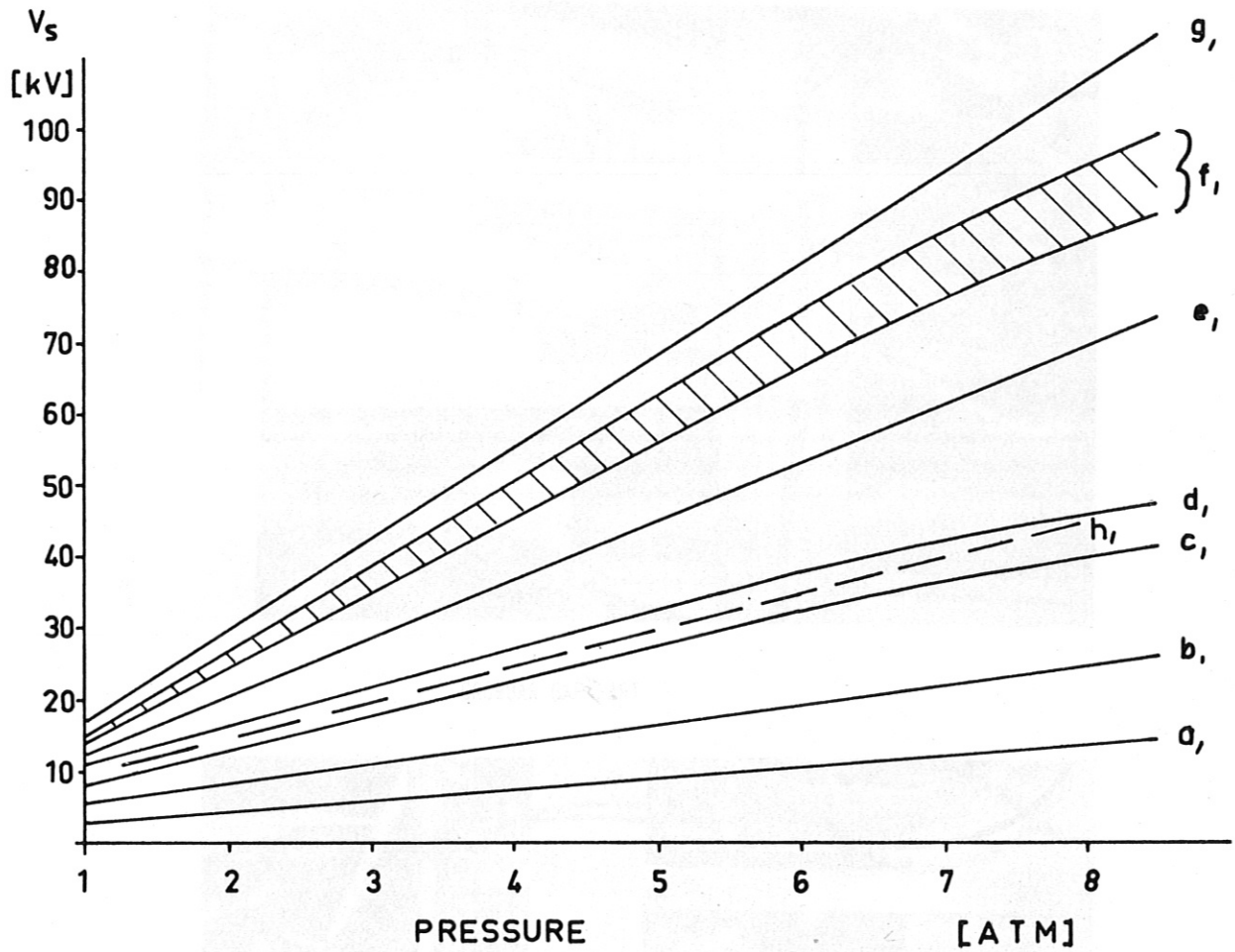

BOTH POLARITIES WITHIN 10%, SHADOWED REGION GIVES SPREAD FOR THE MAIN GAP

a, 1 MM IRRADIATING GAP
b, 1 MM TRIGGER ELECTRODE - MAIN ELECTRODE
c, 2 MM TRIGGER ELECTRODE - MAIN ELECTRODE
d, 3 MM TRIGGER ELECTRODE - MAIN ELECTRODE
e, 3.5 MM CROWBAR GAP
f, 5 MM, 2/3 GAP SPACING MAIN GAP, MEASURED AT 4 UNITS
g, CROWBAR TRIGGER PULSE SHARPENING GAP
h, MIN. WORKING VOLTAGE, JITTER LESS THAN 6 NS ABSOLUTE, DERIVED FROM JITTER DATA

Fig. 11 DC - BREAKDOWN DATA OF SWITCHING UNIT VERSUS PRESSURE

CAPACITORS

TO COLLECTOR

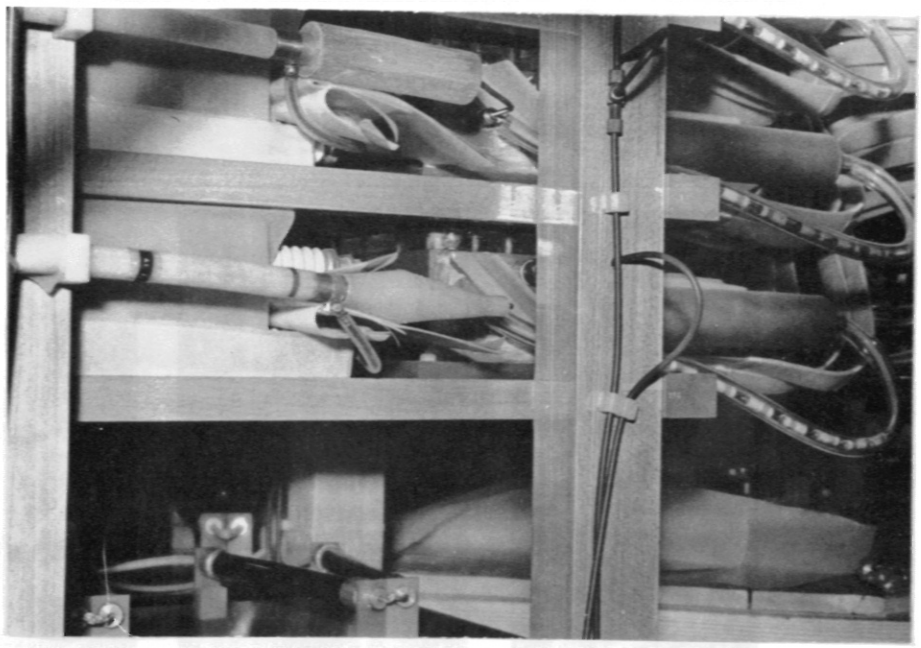

CROWBAR GAP PART

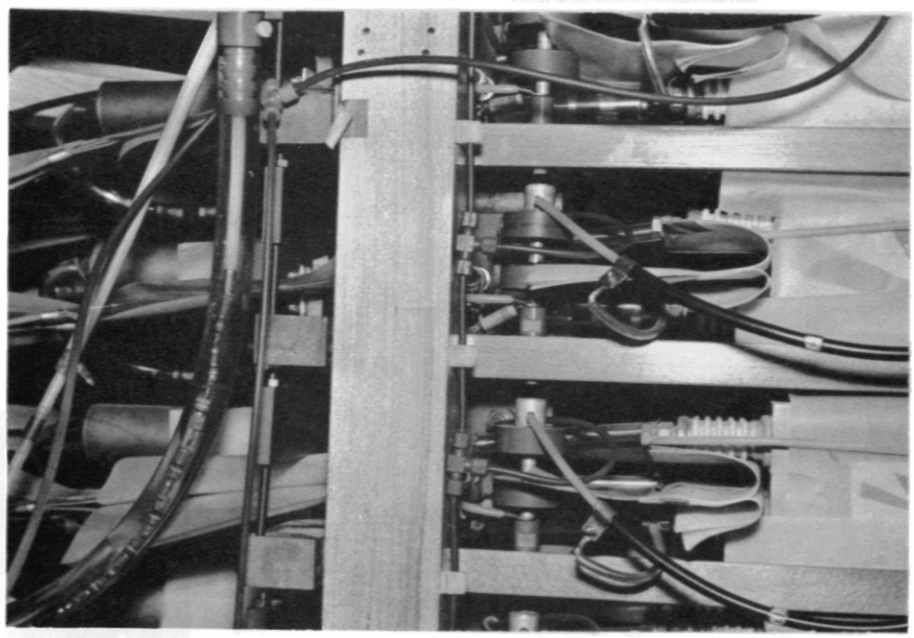

START GAP PART

TO COLLECTOR

CAPACITORS

Fig. 12 SIDE VIEWS OF COMPLETELY INSTALLED SWITCHING UNITS OF TURBULENCE HEATING EXPERIMENT

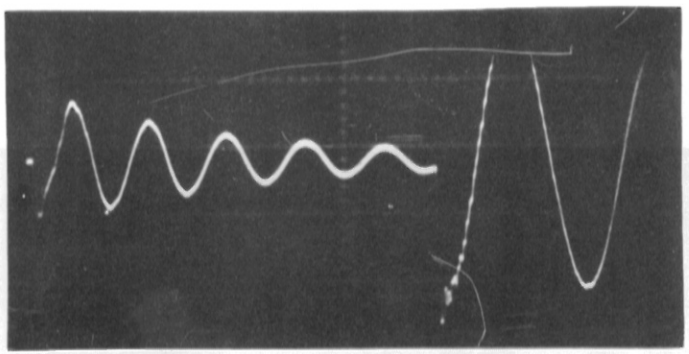

THETA PINCH PREIONISATION 2 x 35 KV, 1 µF AND
MAIN BANK 2 x 40 KV, 5 µF COOPERATION
1 µs/div 5,5 ATM

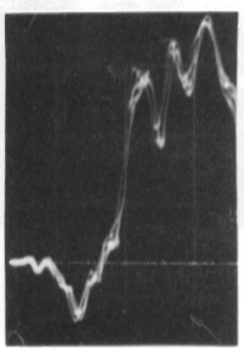

VOLTAGE RISE AT THE COIL
5 DISCHARGES
50 ns/div 14 KV/div

VOLTAGE AT THE LOAD

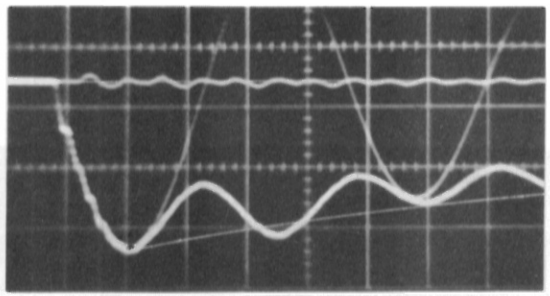

0,5 µs/div 200 KA/div
5 DISCHARGES
T_{crow} = T/4

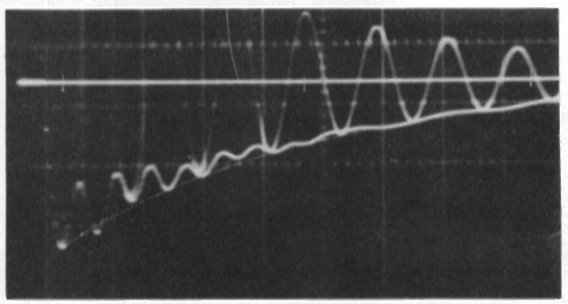

2 µs/div 200 KA/div
T_{crow} = T/4

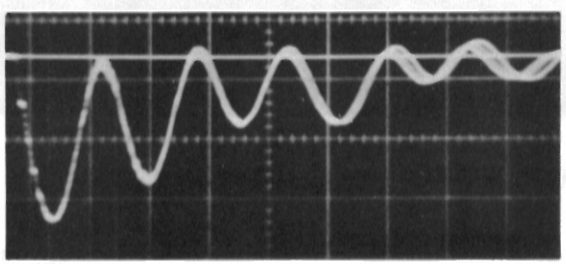

1 µs/div 200 KA/div
T_{crow} = T/2

CURRENT AT THE LOAD

Fig. 13 OPERATION OF 60 SWITCHING UNITS IN THE TURBULENCE HEATING EXPERIMENT

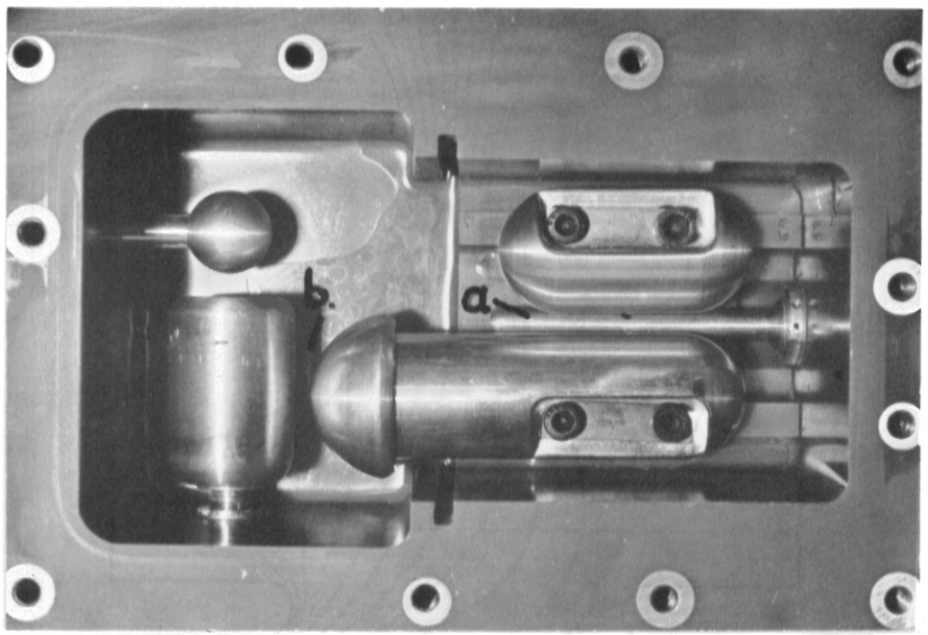

NEW

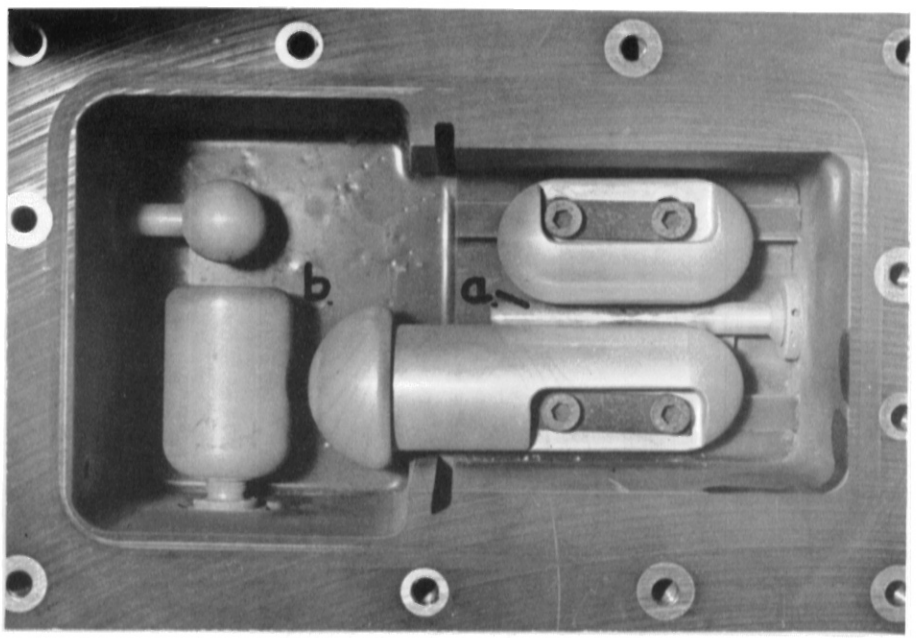

AFTER 3 000 DISCHARGES, ONE YEAR BANK OPERATION

a. START SPARK GAP b. CROWBAR SPARK GAP

Fig. 14 VISIBLE EROSION OF SWITCHING UNIT

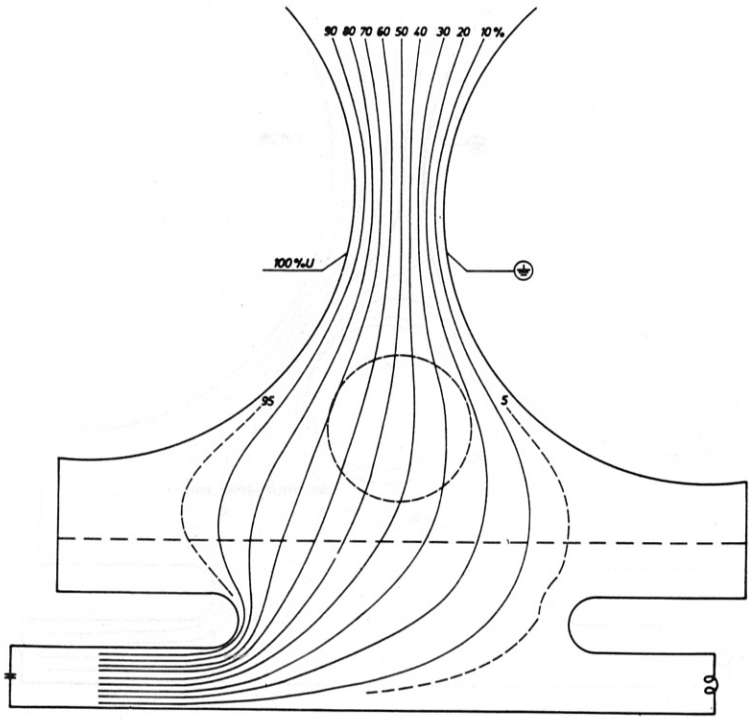

FIG. *15* MAIN FIELD UNDISTURBED BY TRIGGER ELECTRODE

~2.2 U/cm MAXIMUM
~2 U/cm MEAN
} FIELD INTENSITY IN THE SPARK REGION

TRIGGER ELECTRODE AND EPOXY INSULATION MARKED BY BROKEN LINE (NOT CONSIDERED)

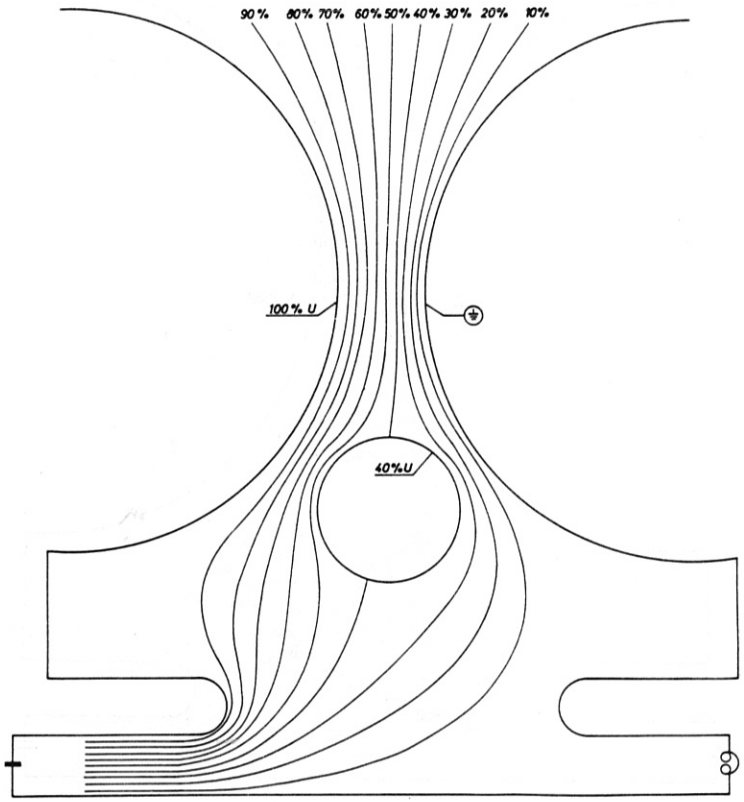

FIG. *16* MAIN FIELD WITH TRIGGER ELECTRODE AT 40% U

~2.5 U/cm MAXIMUM
~2 U/cm MEAN
} FIELD INTENSITY IN THE SPARK REGION

POTENTIAL DIAGRAMS PLOTTED FROM A CARBON PAPER MODEL SIZE 2,5 : 1

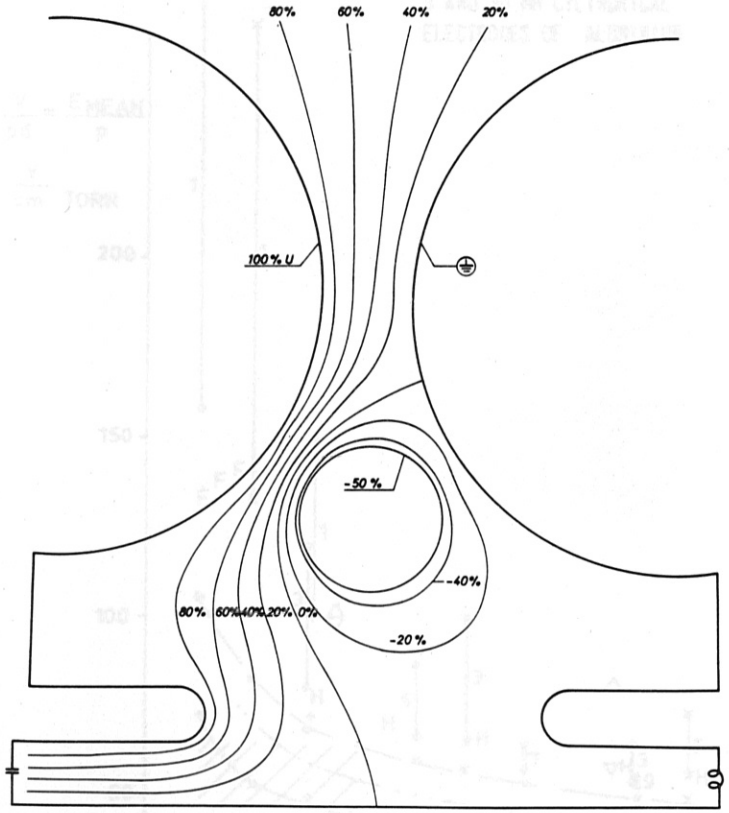

FIG. 17 -50% TRIGGER FIELD, 1. BREAK DOWN STAGE

~ 7 U/cm MAXIMUM
~ 5 U/cm MEAN
} FIELD INTENSITY IN THE SPARK REGION

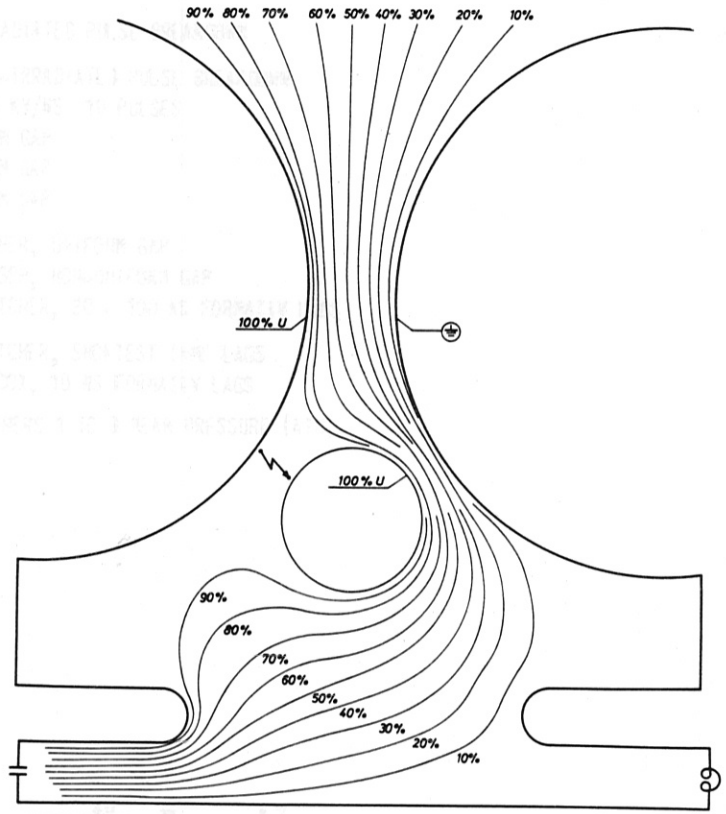

FIG. 18 2. BREAKDOWN STAGE

~ 7 U/cm MAXIMUM
~ 5 U/cm MEAN
} FIELD INTENSITY IN THE SPARK REGION

POTENTIAL DIAGRAMS PLOTTED FROM A CARBON PAPER MODEL SIZE 2,5 : 1

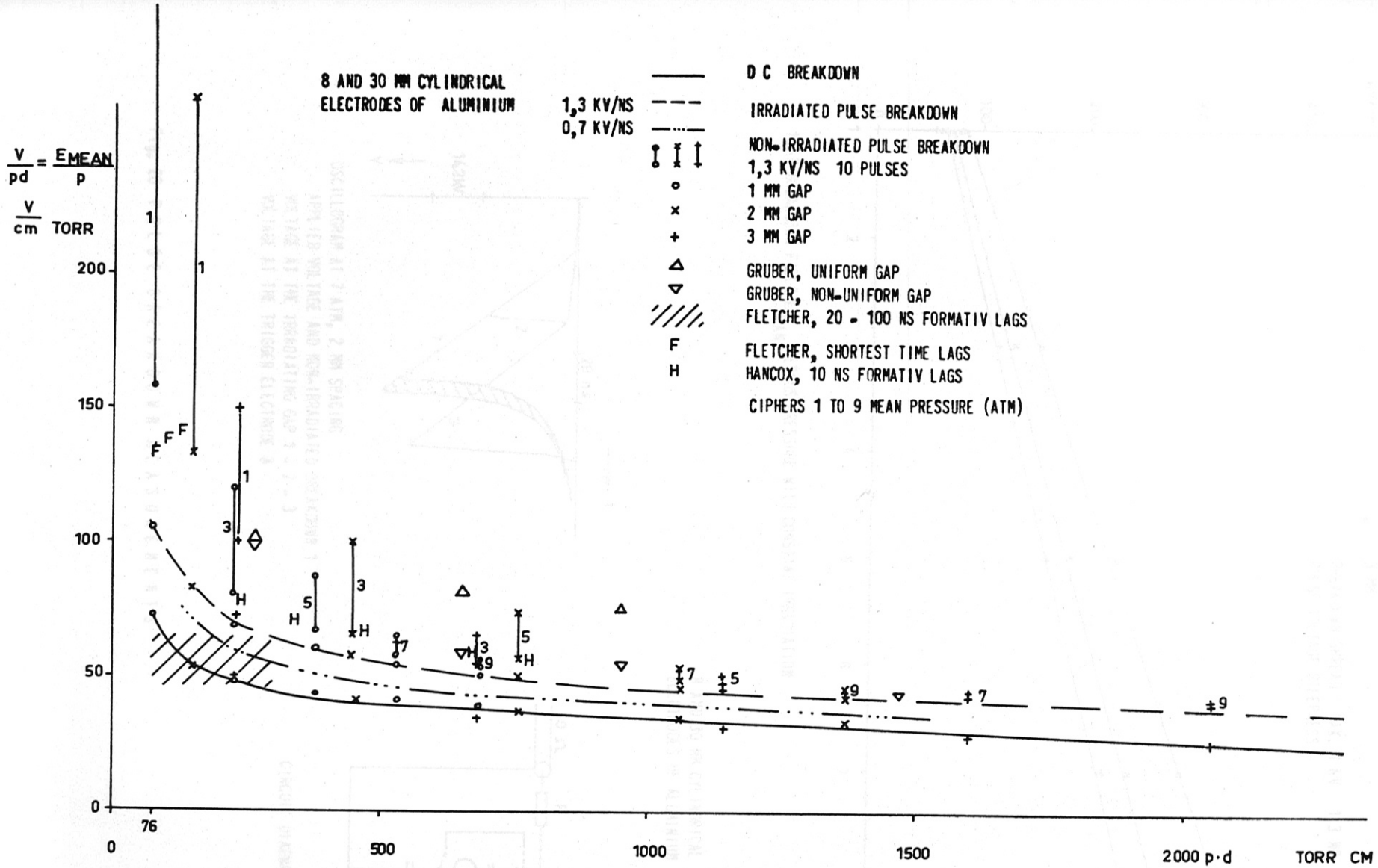

Fig. 19 $V/p.d-E_{MEAN}/p$ VERSUS p.d COMPARED WITH EARLIER DATA

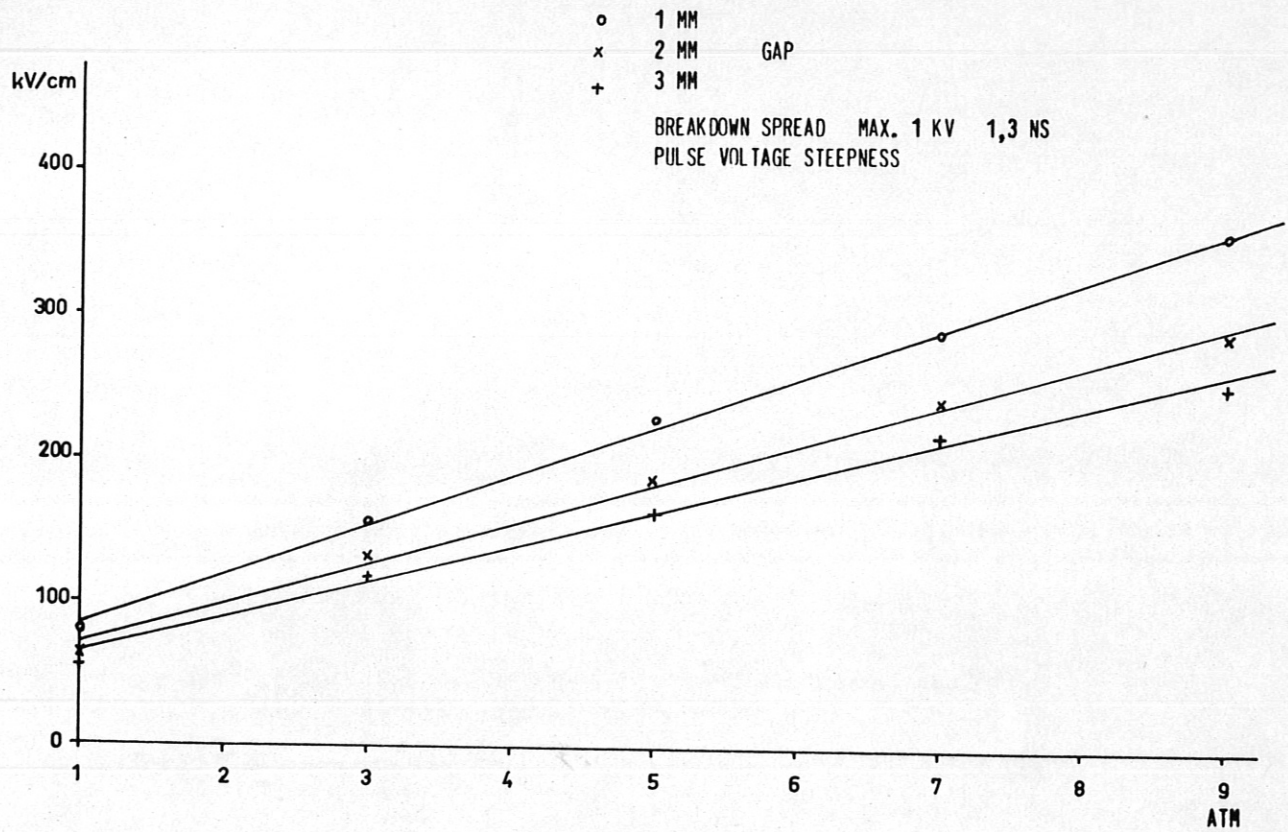

MEAN BREAKDOWN FIELD E_{MEAN} VERSUS PRESSURE WITH CONSTANT IRRADIATION

8 AND 30 MM CYLINDRICAL
ELECTRODES OF ALUMINIUM

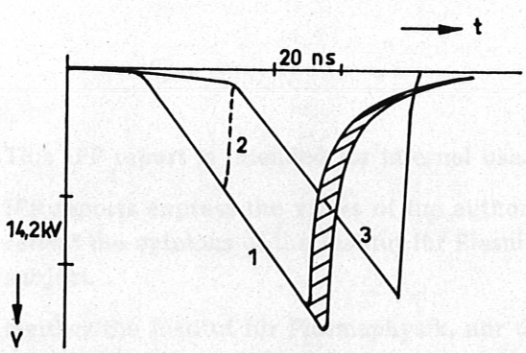

OSCILLOGRAM AT 7 ATM, 2 MM SPACING
APPLIED VOLTAGE AND NON-IRRADIATED BREAKDOWN 1
VOLTAGE AT THE IRRADIATING GAP 1 - 2 - 3
VOLTAGE AT THE TRIGGER ELECTRODE 3

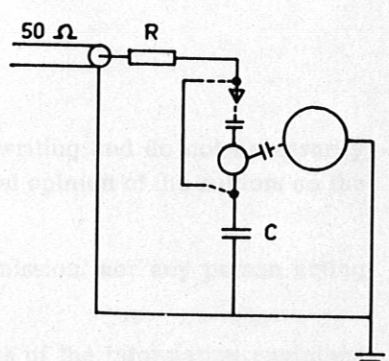

CIRCUIT DIAGRAM

Fig. 20 PULSE BREAKDOWN MEASUREMENTS